Journal of Solid State Chemistry **168,** 457–463 (2002)
doi:10.1006/jssc.2002.9729

Rare-Earth Elements in Molecular Conductors: Crystal and Electronic Structures

Olga N. Kazheva,* Nataliya D. Kushch,* Oleg A. Dyachenko,*,[1] and Enric Canadell†

*Institute of Problems of Chemical Physics, RAS, Chernogolovka, 142432 Moscow Region; Russia; and †Institut de Ciencia de Materials de Barcelona (CSIC), Campus de la UAB, 08193 Bellaterra, Spain

Received December 20, 2001; in revised form March 24, 2002; accepted March 27, 2002

The new molecular conductors with some rare-earth metal-complex anions $(ET)_5[M(NCS)_6NO_3]\cdot C_2H_5OH$ (M = Dy (1), Y (2), Ho (3)) and $(TMTSF)_3[Y(NO_3)_5]\cdot 2C_6H_5Cl$ (4) as well as a new low-temperature modification of tetra-*n*-buthylammonium dysprosium(III) complex, $(Bu_4N)_3[Dy(NCS)_4(NO_3)_2]$ (5) used for the preparation of salt 1 were synthesized and studied by X-ray crystallography at 295 and 110 K. Salts 1–3 have a layered crystal structure with a new packing type of the radical cation layers, called an ω-type. Electronic structure calculations for the compounds 1–3 showed that the paired ET molecules have a positive charge +1 and the single ET molecules are neutral. The directions of the TMTSF stacks in the neighboring organic layers of 4 are practically perpendicular so that salt 4 can be regarded as a precursor of 2D conductors formed by mutually perpendicular directions of conductivity. © 2002 Elsevier Science (USA)

Key Words: **organic conductors; crystal structure; electronic structure; rare-earth elements.**

INTRODUCTION

Most of the known organic conductors and superconductors are radical ion salts based on bis(ethylenedithio)tetrathiafulvalene (ET) and its derivatives involving anionic

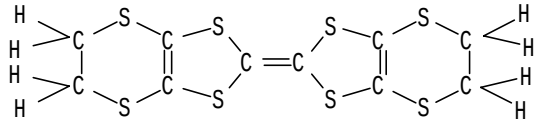

complexes of many metals representing almost all the main periods and groups in the periodic table (1–5). Among these metals, there are Cu, Ag, Au (group I), Zn, Cd, Hg (group II), Ga, In, (group III), Pb (group IV), Bi (group V), Mn, Re (group VII), Fe, Co, Ni, Pd, Pt, Ir (group VIII). It should be stressed that, as an analysis of published data on organic conductors and superconductors shows, the composition and structure of metal-containing anion (the nature of the metal, specific features of its electronic configuration, etc.) have a determining effect on the structure of the conducting layer, thus playing an important role in determining the electroconducting properties of these compounds.

The absence of radically new achievements in this field in the last decade has stimulated both the search of new donors and the widening of the scope of metallocomplex anions used for that purpose. It is natural that lately lanthanides have attracted attention of researchers. An interest to rare-earth elements can be attributed to the intriguing uncertainty of the final result as this metal group has not yet been used to prepare conducting compounds. More importantly, the filling of *f* shells with electrons in the lanthanide series may lead to fundamentally different electroconducting and magnetic properties of synthesized compounds.

Recently, the first series of salts based on organic π-donors and rare-earth 4f ions stable in a wide temperature range have been prepared and investigated: $(BO)_x[Ln(NCS)_6]$, $(TTP)_x[Ln(NCS)_6]$ ($x = 8$) and $(DIEDO)_6[Ln(NCS)_6]$, where Ln = Ho, Er, Yb and Y (6). It should be noted that salts with the same anions but based on ET, $(ET)_4[Ln(NCS)_6]\cdot CH_2Cl_2$, where Ln = Ho, Er, Yb and Y, have proved to be insulators (7). As our investigation has however shown, an introduction of a NO_3 group into the anion improved the conducting characteristics of the compounds. It is confirmed by our published data on synthesis, structure and electroconducting properties of first ET-based semiconductors with Dy- and Y-containing $(ET)_5[M(NCS)_6NO_3]\cdot C_2H_5OH$ complexes (8, 9). Here we would like to report that the use of complex anions of some rare-earth elements led to the successful preparation of new ET salts. This paper

[1]To whom correspondence should be addressed. Fax: 007-096-514-3244. E-mail: doa@icp.ac.ru.

0022-4596/02 $35.00

describes the crystal and electronic band structures of the new $(ET)_5[M(NCS)_6NO_3]\cdot C_2H_5OH$ (M = Dy (**1**), Y (**2**), Ho (**3**)) and $(TMTSF)_3[Y(NO_3)_5]\cdot 2C_6H_5Cl$ (4) salts involving dysprosium, holmium and the nearest analog of rare-earth elements, yttrium, in their composition as well as the investigation of the low-temperature modification of the $(Bu_4N)_3[Dy(NCS)_4(NO_3)_2]$ (5) electrolyte.

EXPERIMENTAL

Synthesis

The new salts **1**–**4** have been prepared by electrochemical oxidation of ET (9, 10). The electrolyte used was the quaternary ammonium salt $(Bu_4N)_3[M(NCS)_4(NO_3)_2]$ (M = Dy, Y, Ho) for conductors **1**–**3** and $(Bu_4N)_3[Y(NO_3)_5]$ for salt **4**. Electrolyte **5** was obtained by known technique (11). The chemical compositions of the salts were determined from X-ray study.

X-Ray Diffraction

An X-ray study of the salts **1**–**3** and electrolyte **5** and has been carried out at 110 K on a Bruker AXS SMART 1000 instrument (12) equipped with a CCD detector (Mo$K\alpha$-line, graphite monochromator, ω scanning, scanning pitch 0.3°, frame measuring time 30 s). An X-ray study of the salt 4 has been carried out at room temperature on the Enraf-Nonius CAD-4 diffractometer with graphite-monochromated Mo$K\alpha$ radiation using $\omega/2\theta$ scanning technique. Crystal data and data collection parameters for salts 1–5 are given in Table 1.

Structure Determination and Refinement

The crystal structures were solved by direct methods and subsequent Fourier syntheses by the SHELXS-97 (13) programs. The structures of **1**–**3** were refined by least squares using an anisotropic (for Dy, Y, Ho and S atoms) and isotropic (for C, N and O atoms) full-matrix approximation by the SHELXL-97 (14) program. The

TABLE 1
Crystal Data and Data Collection Parameters for the $(ET)_5[M(NCS)_6NO_3]\cdot C_2H_5OH$ (M = Dy (1), Y (2), Ho (3)), $(TMTSF)_3[Y(NO_3)_5]\cdot 2C_6H_5Cl$ (4) Salts and $(Bu_4N)_3[Dy(NCS)_4(NO_3)_2]$ (5) Electrolyte

Compound	1 (8)	2 (9)	3	4	5	5 (11)
Empirical formula	$C_{58}H_{46}DyN_7O_4S_{46}$	$C_{58}H_{46}YN_7O_4S_{46}$	$C_{58}H_{46}HoN_7O_4S_{46}$	$C_{42}H_{46}Cl_2N_5O_{15}Se_{12}Y$	$C_{52}H_{108}DyN_9O_6S_4$	$C_{52}H_{108}DyN_9O_6S_4$
Color	Black	Black	Black	Black	Clear-colorless	Clear-colorless
Temperature (K)	110	110	110	295	110	291
M	2542.28	2468.69	2544.71	1968.17	1246.21	1246.21
Symmetry	Monoclinic	Monoclinic	Monoclinic	Monoclinic	Orthorhombic	Orthorhombic
Space group	$P2_1/n$	$P2_1/n$	$P2_1/n$	$C2/c$	$Fdd2$	$Pnnn$
a (Å)	17.670(1)	17.749(2)	17.723(3)	13.491(3)	25.236(2)	12.486(1)
b (Å)	15.548(1)	15.567(2)	15.552(2)	16.849(3)	41.398(3)	12.940(1)
c (Å)	33.002(2)	33.052(2)	33.078(5)	26.495(5)	25.024(2)	21.121(2)
α (deg)	90	90	90	90	90	90
β (deg)	97.858(2)	97.921(2)	97.919(5)	93.20(3)	90	90
γ (deg)	90	90	90	90	90	90
V (Å^3)	8981.7(9)	9045(2)	9030(2)	6013(2)	26143(3)	3412
Z	4	4	4	4	16	2
$D_{calc.}$ (g cm^{-3})	1.880	1.813	1.872	2.174	1.266	1.213
Radiation	Mo$K\alpha$ (λ = 0.71069 Å) graphite monochromated					
μ (Mo$K\alpha$) (mm^{-1})	1.952	1.757	1.990	8.386	1.320	1.265
Scan mode	ω-scanning	ω-scanning	ω-scanning	ω-2θ-scan	ω-scanning	—
θ-range (deg)	1.25–29.88	1.45–30.05	1.45–30.02	2.11–24.98	1.89–30.01	1.50–25.00
Parameters refined	704	704	704	419	650	155
Number of measured reflections	17,054	24,023	18,483	5400	11,997	3014
Number of independent reflections	7329	9791	12,058	5167	8673	—
Number of observed reflections ($F_0 \geq 4\sigma(F_0)$)	4987	7154	5793	3435	4910	1407
Goodness of fit	1.264	1.256	0.928	0.916	0.639	1.01
R	0.078	0.076	0.070	0.045	0.053	0.065
R_w	0.232	0.220	0.206	0.103	0.135	0.090

structure of **4** and **5** were refined by full-matrix least-squares procedures using an anisotropic approximation for all non-hydrogen atoms by the SHELXL-97. Oxygen atoms O(2), O(3) and O(6) in **4** are disordered in two positions with approximately equal population of 0.5. The H atoms in **4** and **5** were calculated. An absorption correction was applied using the SADABS program (15).

Tight-Binding Calculations

The electronic structure of salt **2** (16) was analyzed by carrying out tight-binding extended Hückel-type calculations (17) using a modified Wolfsberg–Helmholz formula (18). Double-ζ Slater-type orbitals were used for C and S and single-ζ Slater-type orbitals for H. The exponents, contraction coefficients and parameters were taken from previous work (19).

DESCRIPTION OF THE CRYSTAL AND ELECTRONIC STRUCTURES AND DISCUSSION

The crystals of salts (**1**–**3**) are isostructural (Table 1). The crystal structure of salts **1**–**3** is characterized by the alternation along the *c*-axis of conducting radical cation layers including ET as well as ethanol molecules, and anionic layers containing the complex units $[M(NCS)_6NO_3]^{4-}$ (M = Dy, Y, Ho) (Fig. 1).

The conducting layers show a clathrate architecture in which groups of four ET pairs form cavities (Fig. 2). The cavities along the *a*- and *b*-axis are uniformly occupied in an alternating way by ET and C_2H_5OH molecules, while the cavities along the *ab* diagonal are occupied by ET molecules only. Note that although the donor layers of the **1**–**3** salts remind those of the well-known κ-phases, first found in the organic superconductors $(ET)_4Hg_3Cl_8$ (20), $(ET)_4Hg_{2.78}Cl_8$ (21) and $(ET)_4Hg_{2.89}Br_8$ (21), in the present case they contain both paired and single ET units (as well as the ethanol molecules).

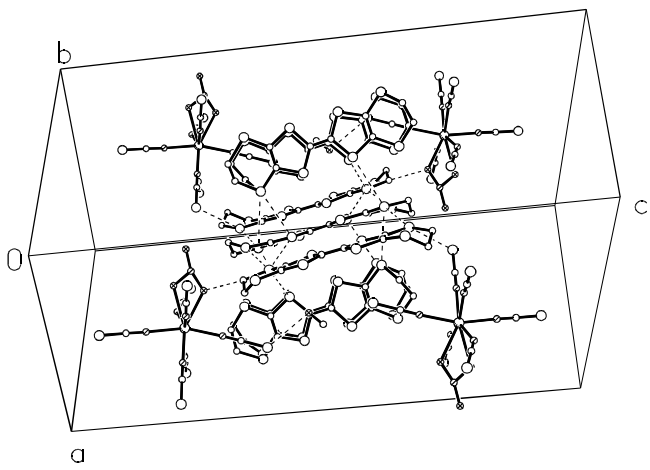

FIG. 1. A fragment of the crystal structure of the $(ET)_5[M(NCS)_6NO_3]\cdot C_2H_5OH$ (M = Dy, Y, Ho) salts.

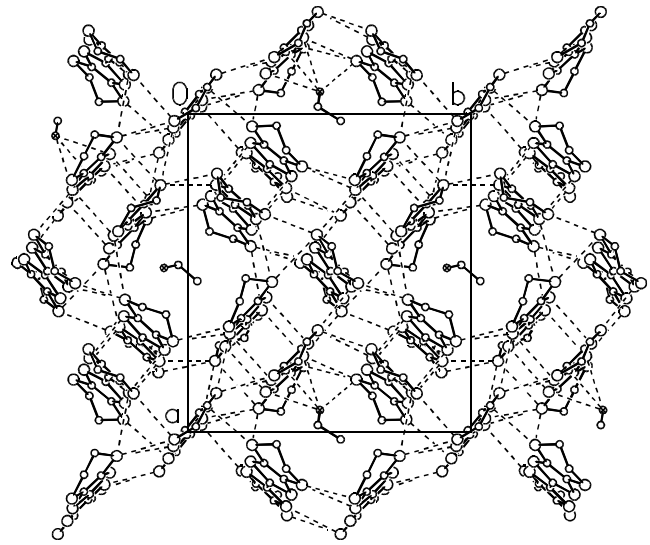

FIG. 2. View of the ω-packing of the ET radical cations in the $(ET)_5[M(NCS)_6NO_3]\cdot C_2H_5OH$ (M = Dy, Y, Ho) salts. The dotted line shows short intermolecular S···S contacts.

Thus, the radical cation layers have a new packing type, earlier unknown (22, 23), which we propose to refer to as ω-type. The conducting layers of salts **1**–**3** exhibit many short S···S contacts in the interval 3.35–3.64 Å between the ET molecules.

The anion layer contains isolated four-charged complex units $[M(NCS)_6NO_3]^{4-}$ (M = Dy, Y, Ho). The M atom of the complex anion is coordinated to six N atoms from NCS groups and one bidentate NO_3 group. Thus, the complex anion can be described as having an approximate pentagonal bipyramidal shape (Fig. 3). As the X-ray analysis data show the obtained radical cation salt **1** includes a $[Dy(NCS)_6NO_3]^{4-}$ anion that is different from a $[Dy(NCS)_4(NO_3)_2]^{3-}$ counterion in the initial electrolyte 5 in its composition ($NCS:NO_3$ groups ratios are 6:1 and 4:2, respectively) and charge (4− and 3−, respectively). To explain this fact, it was assumed that, on dissociation of the $(Bu_4N)_3[Dy(NCS)_4(NO_3)_2]$ electrolyte in the chlorobenzene–ethanol solution, one of the two bidentate NO_3 groups bonded more weakly with a metal atom than NCS groups, is replaced by two NCS groups. However, it must not be fully ruled out that the discovered changes in the anion composition of the initial electrolyte may occur already at the stage of its preparation. To check the latter assumption, we have performed a single-crystal low-temperature X-ray determination of the $(Bu_4N)_3[Dy(NCS)_4(NO_3)_2]$ electrolyte. It should be noted that the interatomic distances and valence angles in the NO_3 groups of **1**–**3** exceed significantly the conventional values

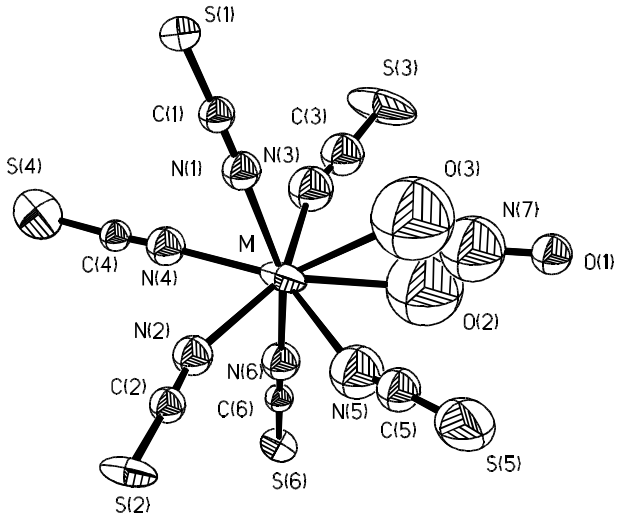

FIG. 3. Structure of the $[M(NCS)_6NO_3]^{4-}$ (M = Dy, Y, Ho) complex anion. Atoms are shown as 50% thermal probability ellipsoids.

(Table 2). The referral of experimental peaks of electron density to the NO_3 group atoms was doubtful. Hence, we tried to identify these peaks as atoms of the NCS group and found in refining of the structure only an insignificant increase of R factor as compared with one for the NO_3 group. However, the N–C and C–S bonds were also quite different from average values. So we preferred the NO_3 group, and the observed geometrical parameters were interpreted as a result of the NO_3 and NCS groups superposition, which can be explained by an uncompleted substitution of the nitrate-groups for the thiocyanate-groups.

A comparison of the main crystal data given in Table 1 shows that depending on temperature the $(Bu_4N)_3[Dy(NCS)_4(NO_3)_2]$ crystals exist in two orthorhombic modifications that differ from each other in symmetry space groups: *Fdd*2 (low-temperature, 110 K) and *Pnnn* (high temperature, 291 K).

Compound **4** shows a layered structure (Fig. 4). In the organic layer, radical cations TMTSF form stacks alternated by chlorobenzene molecules' stacks where the planes of the latter are practically perpendicular to the planes of radical cations TMTSF. In the stacks the radical cations are placed in the following way: (A···B···B···A···B···B) (Fig. 5). The interplanar distances between the A···B and B···B molecules are 3.50 Å, the dihedral angle between the TMTSF planes of different types (A and B) is 1.7°, the cation radicals of B type are parallel to each other. Between TMTSF in stacks we observed short Se···Se contacts 3.708–3.957 Å (the van der Waals radii sum is 4.00 Å (24)). The directions of the TMTSF stacks in the neighboring organic layers are practically perpendicular (Fig. 4). Such a disposition of conducting stacks account for the lack of any visible anisotropy in conductivity usually observed in organic conductors. Since the presence of stacks is usually the optimal situation in order to increase the conductivity, the $(TMTSF)_3[Y(NO_3)_5]\cdot 2C_6H_5Cl$ salt can be regarded as a precursor of 2D conductors formed by 1D conducting layers with mutually perpendicular directions of conductivity. Thus $(TMTSF)_3[Y(NO_3)_5]\cdot 2C_6H_5Cl$ salt can be regarded as a model for crystal engineering of 2D-conductors from 1D conductivity blocks. In general, the creation of a crystal with nD conductivity using n 1D conducting blocks is a novel promising approach in crystal engineering of molecular conductors.

The anion layer is formed by two-charged complexes $[Y(NO_3)_5]^{2-}$, in which Y atom is coordinated by bidentate nitrate groups (Fig. 6) in the form of a trigonal bipyramid. The Y–O and N–O bond lengths are in range from 2.274(7) to 2.535(7) Å and from 1.058(8) to 1.390(8) Å, respectively.

TABLE 2
The Selected Bond Distances and Angles for the $(ET)_5[M(NCS)_6NO_3]\cdot C_2H_5OH$ (M = Dy (1), Y (2), Ho (3)) at 110 K

1		2		3	
Dy–N(1)	2.409(10)	Y–N(1)	2.373(7)	Ho–N(1)	2.378(7)
Dy–N(2)	2.434(11)	Y–N(2)	2.429(6)	Ho–N(2)	2.400(7)
Dy–N(3)	2.432(13)	Y–N(3)	2.406(7)	Ho–N(3)	2.384(8)
Dy–N(4)	2.403(13)	Y–N(4)	2.431(7)	Ho–N(4)	2.443(7)
Dy–N(5)	2.389(16)	Y–N(5)	2.471(9)	Ho–N(5)	2.425(9)
Dy–N(6)	2.366(11)	Y–N(6)	2.349(7)	Ho–N(6)	2.386(7)
Dy–O(2)	2.520(11)	Y–O(2)	2.589(10)	Ho–O(2)	2.589(9)
Dy–O(3)	2.531(11)	Y–O(3)	2.521(9)	Ho–O(3)	2.607(10)
N(7)–O(1)	1.393(11)	N(7–O1)	1.412(8)	N(7)–O(1)	1.385(9)
N(7)–O(2)	1.330(12)	N(7–O2)	1.386(11)	N(7)–O(2)	1.285(11)
N(7)–O(3)	1.365(12)	N(7–O3)	1.407(11)	N(7)–O(3)	1.341(11)
O(1)–N(7)–O(2)	122.8(9)	O(1)–N(7)–O(2)	124.8(7)	O(1)–N(7)–O(2)	125.8(8)
O(2)–N(7)–O(3)	96.3(8)	O(2)–N(7)–O(3)	84.5(7)	O(2)–N(7)–O(3)	87.9(7)
O(1)–N(7)–O(3)	139.3(10)	O(1)–N(7)–O(3)	149.5(8)	O(1)–N(7)–O(3)	146.0(9)

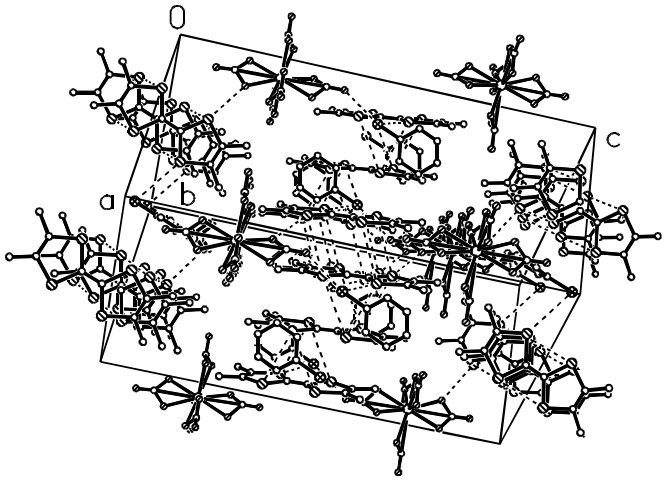

FIG. 4. A fragment of the crystal structure of the $(TMTSF)_3[Y(NO_3)_5]\cdot 2C_6H_5Cl$ salt.

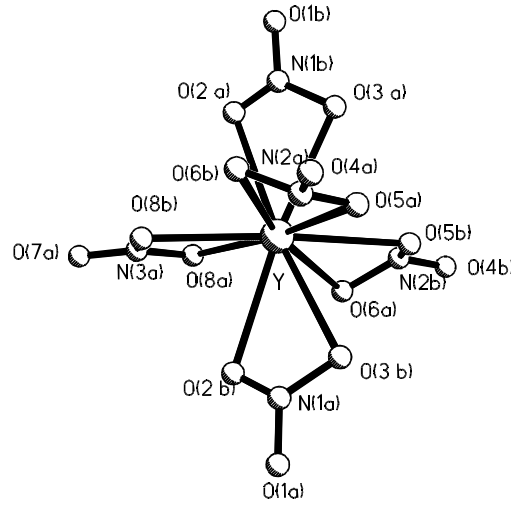

FIG. 6. Structure of the $[Y(NO_3)_5]^{2-}$ complex anion.

At the equatorial plane of the bipyramid, they lie within a range of 2.332(6) –2.444(4), and 1.211(5) –1.390(8) Å, respectively. The NO_3 groups in the apical positions are characterized by the Y–O and N–O bond lengths which range from 2.274(7) to 2.351(7) Å and from 1.058(8) to 1.360(8) Å, respectively.

A short contact O···Se 3.407(7) Å has been found between the O(3) of the anion layer and Se(6) of the cation layer. There are short intermolecular contacts Se···Cl (3.660(2) and 3.822(2) Å) and O···Cl (3.131(5) Å) (the van der Waals radii sum is 3.90 and 3.19 Å, respectively (24)).

The conductivities at room temperature of the $(ET)_5[M(NCS)_6NO_3]\cdot C_2H_5OH$ (M = Dy, Y, Ho) crystals are 0.1–0.2 $\Omega^{-1}cm^{-1}$ and that of the $(TMTSF)_3[Y(NO_3)_5]\cdot 2C_6H_5Cl$ crystals are $10^{-3}\,\Omega^{-1}cm^{-1}$. The **1**–**4** salts exhibit a semiconducting behavior (9, 10).

The repeating unit of a donor layer of salt **2** contains 10 ET donors so that the band structure in the vicinity of the Fermi level contains 10 HOMO bands. The calculated band structure for a donor layer of salt **2** is shown in Fig. 7. Given the stoichiometry and the tetravalent nature of the anion, there must be eight holes in these HOMO bands. As shown in Fig. 7, there is an energy gap between the four upper bands and the lower ones so that, in agreement with the conductivity results, salt **2** should be a semiconductor.

The interaction between the two ET donors of every pair is strong so that the two HOMOs of each of these pairs lead to a low-lying orbital, which we will refer to as $(\Psi^+)_{HOMO}$, and to an upper-lying orbital, which we will refer to as $(\Psi^-)_{HOMO}$. The four upper bands in Fig. 7 are build from the four $(\Psi^-)_{HOMO}$ orbitals associated with the four ET pairs in the repeat unit of the donor layer. The six filled bands of Fig. 7 can be divided into two groups: (a) two very flat bands, at the top of this group of filled bands, which are each associated with the HOMO of one of the

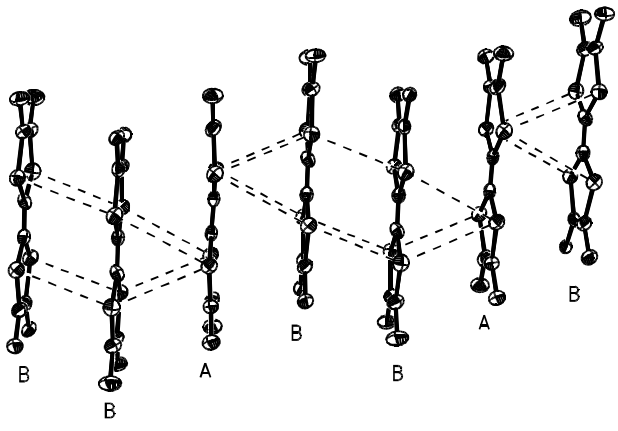

FIG. 5. Packing of conducting layers in the $(TMTSF)_3[Y(NO_3)_5]\cdot 2C_6H_5Cl$ salt.

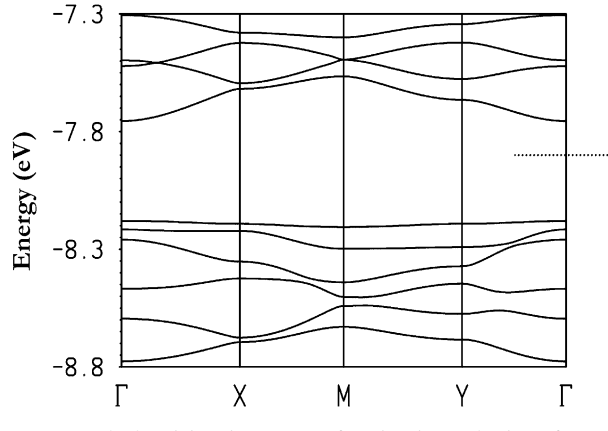

FIG. 7. Calculated band structure for the donor lattice of 2 where the dashed line refers to the Fermi level. Γ = (0, 0), X = (a^*/2, 0), Y = (0, b^*/2) and M = (a^*/2, b^*/2).

single ETs, and (b) four bands, slightly lower in energy, which are build from the $(\Psi^+)_{HOMO}$ orbitals of the four ET pairs. Consequently, since the four empty bands are mostly based on the ET pairs, we can conclude that the paired ET donors must be considered as ET^+ whereas the single ET donors must be considered as ET^0.

At this point, the question arises of how the single ET donors should be considered: as a real part of the donor lattice or as just filling the cavities of the donor lattice build from the ET pairs (i.e., exactly like the C_2H_5OH molecules). As far as the HOMO···HOMO interactions are concerned, this question can be answered by evaluating the so-called $\beta_{HOMO-HOMO}$ interaction energies, which are a measure of the interaction between two HOMOs in adjacent sites of the lattice (25). There are three types of HOMO···HOMO interactions: (a) intra-pair, (b) inter-pair (every ET of one pair interacts with two ETs of adjacent pairs so that every ET pair interacts with four adjacent pairs) and (c) interactions between the single ETs and the paired ones (every single ET makes a total of eight interactions with the eight donors of four adjacent ET pairs). The calculated $\beta_{HOMO-HOMO}$ values for salt **2** are very large for the intra-pair interactions (around 0.8 eV) and quite sizeable for the inter-pair interactions (0.14–0.26 eV). In contrast, of the eight interactions between the single and paired ETs, only one is associated with a sizeable $\beta_{HOMO-HOMO}$ (0.18) whereas the remaining seven are around one order of magnitude smaller. Consequently, these interactions seem to be weak and, as far as the HOMO···HOMO interactions are concerned (i.e., those determining the shape of the band structure around the Fermi level), the ET sublattice of these salts can be described as a series of ET^+ dimers interacting relatively strongly among them but only weakly with single ET^0 units partially filling the cavities of the dimers lattice.

In order to check this conclusion, we have calculated the band structure of the same ET lattice in which we have removed the single ETs. The calculated band structure is very similar to that in Fig. 7 except for the absence of the two upper filled very flat bands associated with the single ETs. However, as far as the band structure of Fig. 7 is correct, it cannot be concluded that the single ETs do not influence the conductivity of the lattice: the holes of these semiconductors are associated with the upper flat bands (i.e., mainly with the HOMOs of the weakly interacting single ETs) and the electrons with the bottom of the more dispersive empty bands (i.e., mainly with the set of interacting $(\Psi^-)_{HOMO}$ orbitals of the ET dimers).

CONCLUSION

In conclusion, the novel radical cation salts $(ET)_5[M(NCS)_6NO_3]\cdot C_2H_5OH$ (M = Dy, Y, Ho) were prepared and their crystal and electronic structures were examined. These salts have radical cation layers with a new packing type (ω-type) separated by anionic layers. Despite the presence of a great number of inter- and intramolecular short S···S contacts in the 2D radical cation layers, the salts exhibit semiconducting properties.

Our investigation of the low-temperature modification of the $(Bu_4N)_3[Dy(NCS)_4(NO_3)_2]$ electrolyte confirms that the composition of the examined compound does not vary in the range 291–110 K. Therefore, the discussed distinction in the anion composition of the $(ET)_5[Dy(NCS)_6NO_3]\cdot C_2H_5OH$ semiconductor (1) as compared to the anion composition in the $(Bu_4N)_3[Dy(NCS)_4(NO_3)_2]$ electrolyte (5) is actually caused by the replacement of one NO_3 group in the electrolyte by two NCS groups and occurs in the course of the electrochemical reaction.

It was found that the directions of the TMTSF stacks in the neighboring organic layers in the $(TMTSF)_3[Y(NO_3)_5]\cdot 2C_6H_5Cl$ salt were practically perpendicular. Since the presence of stacks is usually the optimal situation in order to increase the conductivity, this salt can be regarded as a precursor of 2D conductors formed by 1D conducting layers with mutually perpendicular directions of conductivity. Electronic structure calculations and crystal chemical investigation of the **1–4** structure allowed to conclude that for salts **1–3** the non-metallic (semiconductive) properties were connected with the strong dimerization within the ET pairs, while for compound **4** with a band gap due to the presence of two different TMTSF molecules.

ACKNOWLEDGMENTS

This work was supported by the RFBR (Project 00-03-32809), DGI-Spain (Project BFM2000-1312-C02-01) and Generalitat de Catalunya (1999 SGR 207).

REFERENCES

1. M. Williams, J. R. Ferraro, R. I. Thorn, K. D. Carlson, U. Geiser, H. H. Wang, A. M. Kini, and M.-H. Whangho, Organic superconductors, Prentice-Hall.'' Englewood Cliffs, NJ, 1992.
2. P. Cassoux, L. Valade, H Kobayashi, A. Kobayashi, R. A. Clark, and A. E. Underhill, *Coord. Chem. Rev.* **110,** 115–160 (1991).
3. E. B. Yagubskii, *Mol. Cryst. Liq. Cryst.* **230,** 139–156 (1993).
4. E. B. Yagubskii, *J. Solid State Chem.* **168,** 464–469 (2002).
5. A. Graja and O. Dyachenko, *Macromol. Symp.* **104,** 223–249 (1996).
6. M. Tamura, K. Yamanaka, Y. Mori, Y. Nishio, K. Kajita, H. Mori, S. Tanaka, J.-I. Yamaura, T. Imakubo, R. Kato, Y. Misaki, and K. Tanaka, ''Proceedings. of ICSM2000,'' Gastein, Austria, 2000.
7. M. Tamura, F. Matsuzaki, Y. Nishio, K. Kajita, T. Kitazawa, H. Mori, and S. Tanaka, *Synth. Met.* **102,** 1716–1717 (1999).
8. O. A. Dyachenko, O. N. Kazheva, V. V. Gritsenko, and N. D. Kushch, *Synth. Met.* **120,** 1017–1018 (2001).
9. O. N. Kazheva, N. D. Kushch, G. G. Aleksandrov, and O. A. Dyachenko, *Mater. Chem. Phys.* **73,** 193–197 (2001).

10. N. D. Kushch, O. N. Kazheva, V. V. Gritsenko, L. I. Buravov, K. V. Van, and O. A. Dyachenko, *Synth. Met.* **123,** 171–177 (2001).
11. D. F. Mullica, B. M. Bonilla, M. C. David, J. M. Farmer, and J. A. Kautz, Inorg. *Chim. Acta* **292,** 137–143 (1999).
12. SMART (control) and SAINT (integration) Software, Version 5.0 Bruker AXS Inc., Madison, WI, 1997.
13. G. M. Sheldrick, "SHELXS-97. Program for the Solution of Crystal Structures." University of Göttingen, Germany, 1997
14. G. M. Sheldrick, "SHELXL-97. Program for the Refinement of Crystal Structures." University of Göttingen, Germany, 1997
15. G. M. Sheldrick, "SADABS, Program for Scaling and Correction of Area Detector Data." University of Gottingen, Germany, 1997.
16. O. N. Kazheva, M. Gener, V. V. Gritsenko, N. D. Kushch, E. Canadell, and O. A. Dyachenko, *Mendeleev Commun.* **11,** 182–184 (2001).
17. M.-H. Whangbo and R. Hoffmann, *J. Am. Chem. Soc.* **100,** 6093–6098 (1978).
18. J. Ammeter, H.-B. Bürgi, J. Thibeault, and R. Hoffmann, *J. Am. Chem. Soc.* **100,** 3686–3692 (1978).
19. A. Pénicaud, K. Boubekeur, P. Batail, E. Canadell, P. Auban-Senzier, and D. Jérome, *J. Am. Chem. Soc.* **115,** 4101–4112 (1993).
20. R. N. Lyubovskaya, R. B. Lyubovskii, R. P. Shibaeva, M. Z. Aldoshina, L. M. Goldenberg, L. P. Rosenberg, M. L. Khidekel, and Ju. F. Shulpyakov, JETP Lett. **42,** 380–391 (1985).
21. R. N. Lyubovskaya, E. I. Zhilyaeva, S. I. Pesotskii, R. B. Lyubovskii, L. O. Atovmyan, O. A. Dyachenko, and T. G. Tahkirov, *JETP Lett.* **46,** 188–197 (1987).
22. T. Mori, H. Mori and S. Tanaka, *Bull. Chem. Soc. Jpn.* **72,** 179–197 (1999).
23. T. Mori, *Bull. Chem. Soc. Jpn.* **71,** 2509–2526 (1998).
24. Yu. V. Zefirov, *Krystallografiya.* **42,** 936–958 (1997).
25. M.-H. Whangho, J. M. Williams, P. C. W. Leung, M. A. Beno, T. J. Emge, and H. H. Wang, *Inorg. Chem.* **24,** 3500–3502 (1985).